J. Electroanal. Chem., 238 (1987) 277–295
Elsevier Sequoia S.A., Lausanne – Printed in The Netherlands

ELECTROGENERATED CHEMILUMINESCENCE

PART XLVIII. ELECTROCHEMISTRY AND ELECTROGENERATED CHEMILUMINESCENCE OF BIS(2,4,6-TRICHLOROPHENYL) OXALATE–LUMINESCER SYSTEMS

ROSSELLA BRINA and ALLEN J. BARD
Department of Chemistry, The University of Texas, Austin, TX 78712 (U.S.A.)

(Received 27th March 1987; in revised form 8th July 1987)

ABSTRACT

The electrochemical behavior and electrogenerated chemiluminescence (ECL) of bis(2,4,6-trichlorophenyl) oxalate (TCPO) in acetonitrile + benzene (2:1 v/v) solutions have been investigated. Quasi-reversible one-electron reduction of TCPO occurs, and the reduction product, the anion radical $TCPO^{\cdot-}$ (in the absence of O_2), is stable on the cyclic voltammetric time scale. In the presence of oxygen, $TCPO^{\cdot-}$ and $O_2^{\cdot-}$ react, ultimately producing trichlorophenoxide ion and CO_2. ECL is observed on reduction of TCPO + O_2 solutions containing a luminescent compound (e.g., 9,10-diphenylanthracene) where the ECL spectrum is typical of the luminescer. No ECL is observed in the absence of O_2 during reduction of TCPO and fluorescer. The ECL only appears with trace amounts of O_2, suggesting that this system might be useful as a detector for very low concentrations of O_2.

INTRODUCTION

Since the discovery of the first peroxyoxalate chemiluminescent system [1] based on the oxalyl chloride–hydrogen peroxide reaction in the presence of a fluorescer, e.g., 9,10-diphenylanthracene (DPA), chemiluminescent reactions of many oxalic acid derivatives under conditions analogous to the oxalyl chloride system have been reported [2–4]. In peroxyoxalate chemiluminescence the emission spectrum is that of the added fluorescer [5]. In the mechanism proposed by Rauhut et al. [3], Scheme 1, the nucleophilic attack of hydrogen peroxide leads to the peroxyoxalic acid, the precursor of the key intermediate, 1,2-dioxetanedione (**2**), which forms a charge transfer complex with the fluorescer. The decomposition of this charge transfer complex yields the first excited singlet-state of the fluorescer, which emits the light. However, there is no direct spectral nor chemical evidence of the existence of the dioxetanedione intermediate [2,6]. According to Lechtken and Turro [7], this inter-

0022-0728/87/$03.50

SCHEME 1

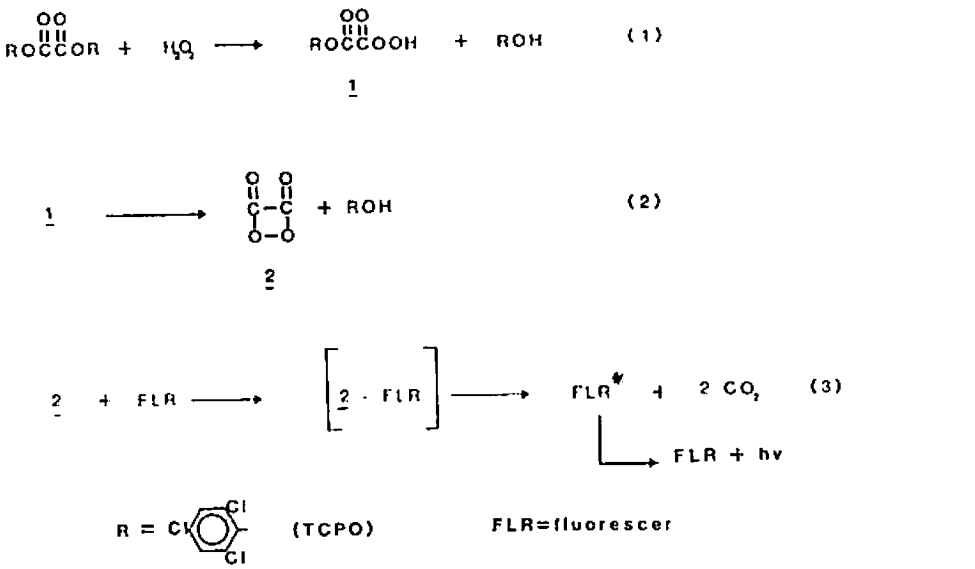

mediate can transfer an amount of energy equivalent to 439 kJ/mol (≡ 272 nm), and the chemiluminescence intensity, once corrected for the fluorescence quantum yield, decreases with an increase in the fluorescer's singlet excitation energy. McCapra [8] suggested a CIEEL-type mechanism (chemically induced electron exchange luminescence) [9] for the peroxyoxalate reaction, where the intermediate accepts an electron from the fluorescer, as shown in Scheme 2. According to this mechanism, the fluorescers which are the best electron donors will be the most efficient in the peroxyoxalate system [2]. Similar ECL processes have been observed during the oxidation of luminescers (e.g., DPA, $Ru(bpy)_3^{2+}$) in the presence of

SCHEME 2

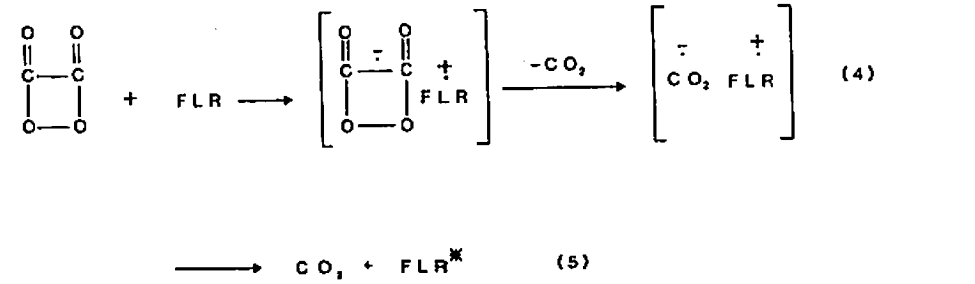

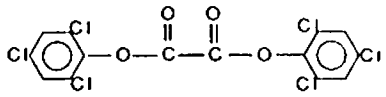

TCPO

oxalate ion, where the intermediacy of $CO_2^{\cdot-}$ is invoked [10]. Because these reactions show high quantum efficiencies [3,11], peroxyoxalate chemiluminescence has found many analytical applications, particularly in hydrogen peroxide determinations [12], and in determination of polycyclic aromatic hydrocarbons [13] and fluorescent-labeled substrates [14]. Polycyclic aromatic hydrocarbons emitting in the visible and infrared region can be excited by the peroxyoxalate system [6,15] with weaker excitation of fluoresceers emitting in the UV region [16] in agreement with the energetic considerations already mentioned.

We report here studies of the electrochemistry and ECL of the oxalate ester bis(2,4,6-trichlorophenyl) oxalate (TCPO).This ester has been widely used in chemiluminescence studies because of its ease of preparation [17], stability and high quantum yield [6], although the exact details of the reaction mechanism are still under investigation [18]. A problem with most analytical applications of oxalate ester chemiluminescence is the instability of the oxalic acid derivative in the final solution, when a fairly high percentage of water, together with hydrogen peroxide and decomposition products, are present [19]. TCPO, like other oxalic acid derivatives, is not very soluble or stable in water [20], and peroxides and 2,4,6-trichlorophenol (TCP), one of the TCPO decomposition products, are other sources of instability. Improvements in TCPO stability could be achieved by generating the superoxide ion in situ, e.g., electrochemically, in a non-aqueous solvent. There have been few studies of the electroreduction of oxalate esters [21]. Some studies on the electrochemical reduction of dialkyl and diphenyl oxalate esters to the radical anions in non-aqueous solvent have been reported [22,23], but no information is available on the electrochemical behavior of the oxalate esters used for peroxyoxalate chemiluminescence.

EXPERIMENTAL

Chemicals

TCPO (Chemical Dynamics Corp., South Plainfield, NJ) was recrystallized twice from ethyl acetate and dried under vacuum (m.p. 194°C). 2,4,6-Trichlorophenol (TCP) (98%, Aldrich Chemical Co., Milwaukee, WI) was recrystallized from ethyl acetate and dried under vacuum. 9,10-Diphenylanthracene (DPA) (gold label, Aldrich) and rubrene (Aldrich) were crystallized from ethanol + benzene (1 : 1 v/v) and dried under vacuum. $Ru(bpy)_3(PF_6)_2$ was prepared from the dichloride salt (Strem Chemicals, New Buryport, MA), recrystallized from ethanol + water and dried under vacuum. The supporting electrolyte used was tetra-n-butylammonium tetrafluoroborate ($TBABF_4$, Southwestern Analytical Chemicals, Austin, TX).

$TBABF_4$ was recrystallized three times from ethyl acetate and dried under vacuum. Benzene (Spectroanalyzed, Fisher Scientific, Fair Lawn, NJ) was dried over activated Woelm Alumina N-Super I (Woelm Pharma, West Germany) for 24 h under vacuum. Acetonitrile (HPLC grade, Fisher Scientific) was distilled from calcium hydride over Woelm Alumina B-Super I. The solvent used in all the electrochemical and ECL measurements was a mixture of acetonitrile and benzene (2 : 1 v/v). The solvent mixture was transferred into the cell on a vacuum line, by the vapor transfer method. Freshly purified solvents were used each time. The solutions were degassed by at least three freeze–pump–thaw (f–p–t) cycles before each experiment. Oxygen additions were made by bubbling the gas through the solution with stirring. After each addition, the cell was sealed again.

Apparatus

Electrochemical measurements were performed in a conventional three-electrode cell, with an optically flat bottom. The working electrode was a platinum disk electrode (0.02 cm^2) with the surface parallel to the bottom of the cell. The auxiliary electrode was a platinum gauze, and the reference electrode was a silver wire quasi-reference electrode (qre), housed in a small fritted compartment. A conventional three compartment cell was used for coulometric experiments. All cells were provided with connections for the vacuum line. Electrochemical and ECL experiments were carried out using a Princeton Applied Research (PAR) model 173 potentiostat, a model 175 universal programmer and a model 179 digital coulometer. Current–potential curves were recorded on a Houston Instruments model 2000 X–Y recorder or a Norland model 3001 digital oscilloscope. Ecl emission intensities were detected with an Aminco-Bowman spectrophotofluorometer employing a Hamamatsu R928 photomultiplier tube. The ESR cell described [24] was adapted for measurements under vacuum.

RESULTS AND DISCUSSION

Voltammetric measurements under vacuum

Figure 1a shows a typical cyclic voltammogram (CV) of TCPO in AN + benzene (2 : 1 v/v) solution containing 0.1 *M* $TBABF_4$ as supporting electrolyte under vacuum (rigorously O_2-free conditions) at a scan rate (v) of 100 mV/s, at a platinum disk electrode. A cathodic wave (I) was observed at −1.16 V vs. Ag qre, which showed an anodic wave (III) on scan reversal (Fig. 1c). A second irreversible reduction wave (II) at −2.56 V vs. Ag qre and an anodic irreversible oxidation wave (IV) at +0.52 V vs. Ag qre were also observed. Wave (IV) increased significantly when the negative scan was extended to include wave (II). Figure 1d shows a CV of 0.1 *M* $TBABF_4$ solution in AN + benzene (2 : 1 v/v) containing 5 m*M* of TCP (a proposed product in the reaction scheme as described below) under vacuum. An irreversible reduction wave (V) at −1.3 V and an irreversible oxidation wave (VI) at +0.52 V are observed. The peak potentials were determined vs. the ferricinium/ferrocene couple, which showed a reversible wave at +0.50 V vs. Ag qre in the same

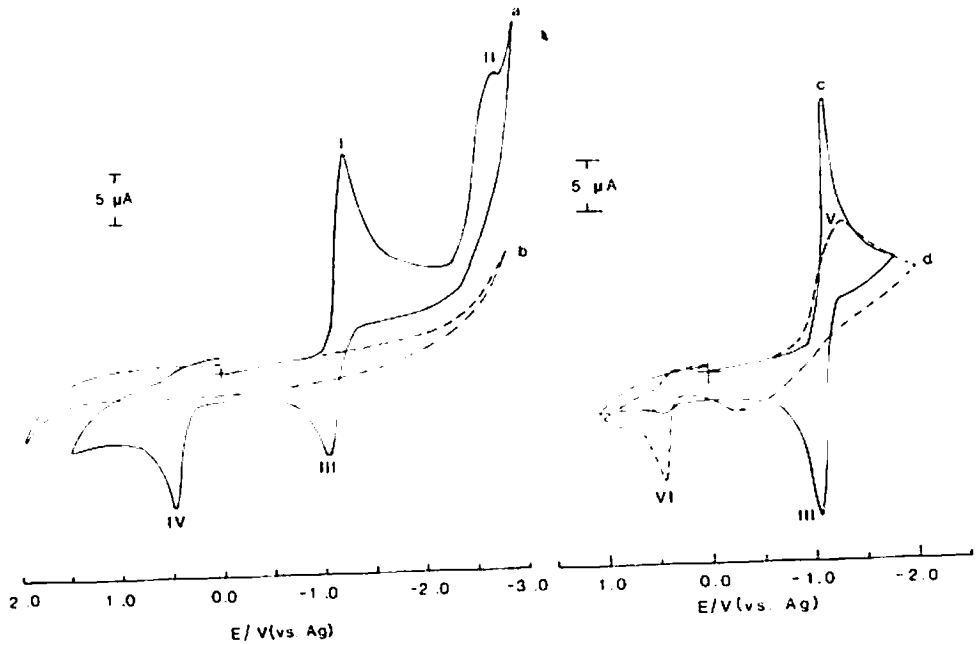

Fig. 1. (a) Cyclic voltammogram of 5 mM TCPO in AN + benzene (2:1 v/v) + 0.1 M $TBABF_4$, under vacuum. Scan rate, 100 mV s^{-1}; Pt disk (0.020 cm^2). (b) CV of 0.1 M $TBABF_4$ in AN + benzene (2:1 v/v) under vacuum; scan rate 100 mV s^{-1}. (c) As (a) with scan reversed ca. 500 mV after first reduction peak. (d) CV of 5 mM TCP in AN + benzene (2:1 v/v) + 0.1 M $TBABF_4$, under vacuum; scan rate, 100 mV s^{-1}.

solution. The data concerning wave (II), wave (IV), and TCP will be discussed later. The values of the peak current ratio of the anodic wave (III) to the cathodic wave (I) (i_{pa}/i_{pc}), the peak potential separation (ΔE_p) and the current function $i_{pc}/(v^{1/2}c)$ are shown in Table 1. In these measurements the potential was reversed 200 mV past the peak potential E_{pc} of wave (I). The ratio i_{pa}/i_{pc} at different scan rates was close to unity, showing that on this time scale the reduction product is stable. When positive feedback was used to compensate for solution resistance, the peak potential separation ΔE_p between wave (I) and (III), at scan rate of 20 mV/s, was 70 mV, as it was for the ferricinium/ferrocene couple in the same solution, showing that some uncompensated resistance effects are included in the measured potentials. Figure 2 shows the plot of the peak potential E_{pc} for wave (I) vs. log v. These cyclic voltammetric results indicate that TCPO is reduced nearly reversibly at a platinum disk electrode in AN + benzene solution under vacuum at slow scan rates with a formal potential $E^{\circ\prime}$ of -1.12 V vs. Ag qre (-1.62 V vs. Fc/Fc^+). To characterize this reduction reaction more quantitatively, chronoamperometric and coulometric experiments were carried out. In the chronoamperometric experiment, the potential was stepped from 0.0 V to -1.45 V vs. Ag qre, and currents (i) in the time (t)

TABLE 1

Cyclic voltammetric results for TCPO under vacuum[a,b]

Scan rate v/V s^{-1}	$i_p v^{-1/2} c^{-1}$/μA s$^{1/2}$ V$^{-1/2}$ mM^{-1}	i_{pa}/i_{pc}	ΔE_p[c]/ mV	$(E_p - E_{p/2})$/ mV
0.02	19.2	1.05	70	70
0.05	19.4	1.0	80	75
0.1	18.3	1.0	90	70
0.2	16.1	1.03	105	85
0.5	15.4	1.02	110	90
1	16.2	1.04	120	94
2	14.4	1.02	252	125
5	14.4	1.04	415	126

[a] The solution was 4 mM TCPO and 0.1 M $TBABF_4$ in AN + benzene (2:1 v/v).

[b] Scan reversed 200 mV after E_{pc}.

[c] IR compensation used.

interval between 10^{-4} and 2 s were plotted vs. $t^{1/2}$. This plot gives a straight line with a correlation coefficient of 0.999. Introducing the slope of this line in the Cottrell equation [25a] leads to a diffusion coefficient of the electroactive species of 1.1×10^{-5} cm^2/s with $n = 1$. Taking the ratio between the cyclic voltammetric $i_p/v^{1/2}$ value at scan rates where the system behaves nearly reversibly and the chronoamperometric $it^{-1/2}$ product yields an n value, the number of electrons in the reduction reaction, of 0.96.

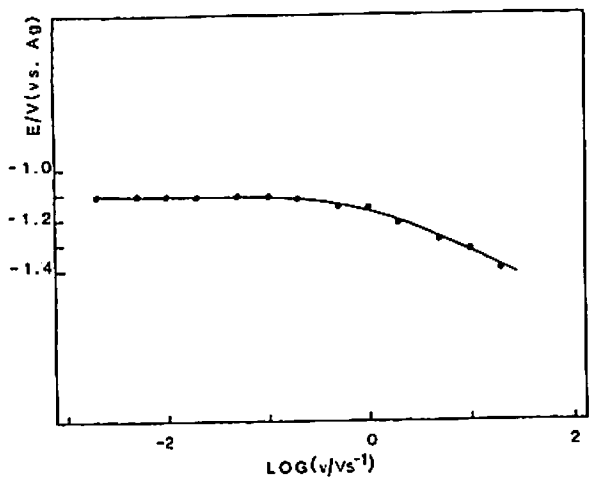

Fig. 2. Variation of the peak potential for TCPO reduction with log scan rate.

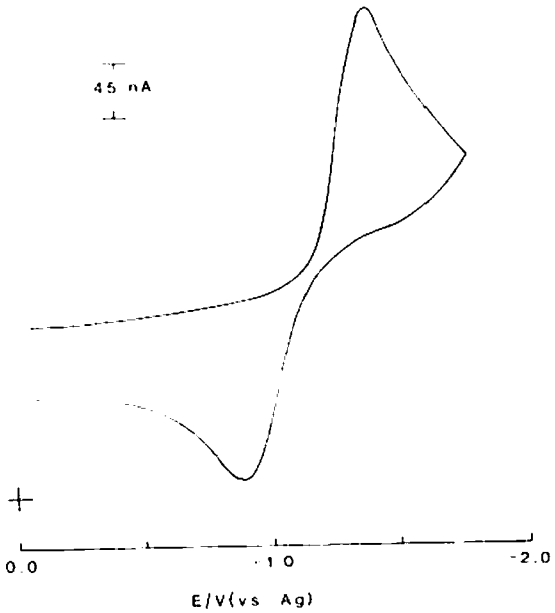

Fig. 3. Cyclic voltammogram of 9 mM TCPO in AN + benzene (2:1 v/v) + 0.2 M $TBABF_4$, under vacuum. Scan rate, 50 V s^{-1}; Pt disk 25 μm diameter.

Ultramicroelectrode studies

To eliminate effects of uncompensated resistance and to obtain a better idea about the heterogeneous kinetics of the electrode reaction, an ultramicroelectrode experiment [26] was performed in a 9 mM TCPO solution containing 0.2 M $TBABF_4$ under vacuum. The working electrode was a platinum disk, 25 μm diameter, and the potential was scanned from 0 to -1.8 V vs. Ag qre. The CV recorded at 50 V/s is shown in Fig. 3. A plot of the cathodic peak current (i_{pc}) for the TCPO reduction peak vs. $v^{1/2}$ over the range 10 to 200 V/s, gave a straight line with a correlation coefficient of 0.999 and a slope that was within 3% from the expected value for totally irreversible behavior ($\Delta E_p > 305$ mV). Under these conditions, the plot of the peak potential E_{pc} vs. ln $v^{1/2}$ allows the determination of the heterogeneous rate constant $k°$ [25b] for the reaction under study. The difference between the peak potential and the half-peak potential leads to an estimate of the transfer coefficient, α. From the ultramicroelectrode results, we obtain $\alpha = 0.4$ and $k° = 0.03$ cm/s for TCPO reduction.

Bulk electrolysis

Coulometric experiments led to an n_{app} value of 0.98, after 3 h electrolysis of a TCPO solution in AN + benzene under vacuum, at -1.5 V vs. Ag qre. However, the reduced form of TCPO appeared to be unstable on the coulometric time scale. A

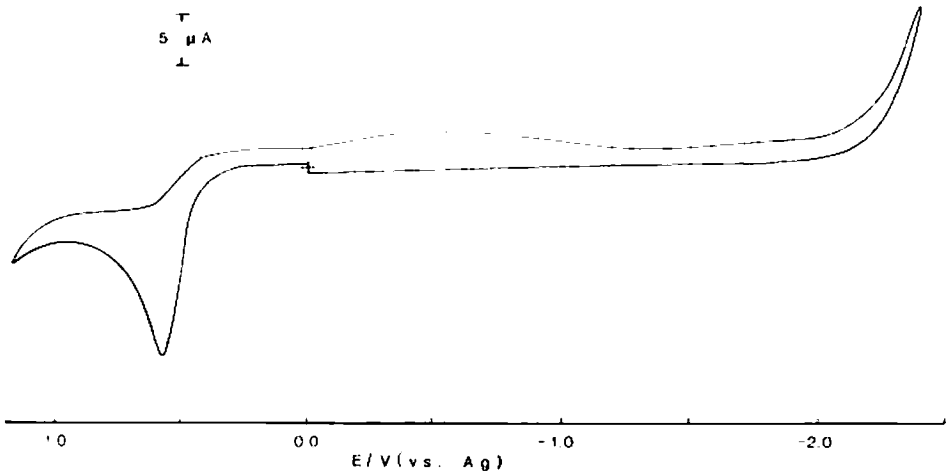

Fig. 4. Cyclic voltammogram after electrolysis of a 3 m*M* TCPO solution in AN + benzene (2:1 v/v) + 0.1 *M* $TBABF_4$, under vacuum at a platinum electrode at −1.5 V vs. Ag qre. Scan rate, 100 mV s^{-1}.

TCPO solution under vacuum is always colorless, while a color change was observed as soon as the bulk electrolysis was started. The solution turned pink and the color intensity increased as the electrolysis proceeded. A second color change, from dark pink to golden yellow, occurred later. This color persisted until the end of the electrolysis and was the final color of the solution. A CV recorded after coulometry (Fig. 4) showed the absence of the TCPO waves and a considerable increase of the irreversible anodic wave observed in Fig. 1a,c at +0.52 V vs. Ag qre. This irreversible anodic wave at +0.52 V is attributed to the oxidation of 2,4,6-trichlorophenoxide in AN + benzene solution (2:1 v/v) under vacuum (Fig. 1d, wave VI). In neither TCPO nor TCP solutions does this wave appear when the electrode is first scanned to positive potentials, showing that the wave in both cases is the result of the oxidation of a species generated during the negative scan. For the TCP solution, we assign the anodic wave at +0.52 V to the oxidation of the 2,4,6-trichlorophenoxide ion produced on reduction of TCP, as discussed below. The solution obtained from TCPO electrolysis at −1.5 V was analyzed to determine the species present. Evaporation of the solvent left a yellow product that turned white after washing with benzene. After separation from the supporting electrolyte, the solid was analyzed by IR and NMR spectroscopies. The NMR spectrum of the electrolysis products is shown in Fig. 5. The spectra revealed the presence of trichlorophenoxide (1) and tetra-n-butylammonium (2) ions.

The mechanism of the slow decomposition reaction of $TCPO^{\cdot -}$ is not known. The loss of the phenoxide would lead to a very reactive species that could perhaps oxidize solvents or the phenoxide itself; since $n_{app} \approx 1$, further reduction at the electrode is apparently unimportant. However, we were unable to detect any other decomposition products in this study. An ESR experiment with in situ generation of

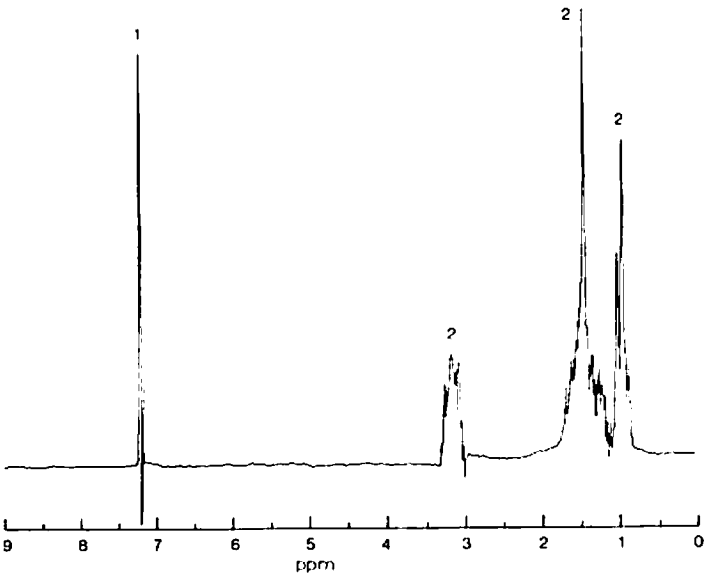

Fig. 5. 200 MHZ proton NMR spectrum of the product of TCPO electrolysis at −1.5 V vs. Ag qre. Tetramethylsilane as standard (0.0 ppm) in $CDCl_3$ solution.

TCPO anion radical was performed by electrolysis of a TCPO solution in AN + benzene under vacuum at −1.6 V vs. Ag qre, at room temperature. The spectrum obtained under these conditions is shown in Fig. 6. A g value of 2.0127 ± 0.0008 was obtained.

Figure 1a,c showed the presence of an irreversible anodic wave at +0.52 V vs. Ag qre. If the potential scan is reversed before −2.0 V (before wave II, Fig. 1c), this anodic wave is very small and the current function decreases at the higher scan rates, showing that the small wave is related to the reaction of $TCPO^{\cdot -}$ generated in wave I with an impurity. (This is discussed in the next section.) When the negative scan is extended beyond the irreversible cathodic wave II, at −2.52 V, the CV shows a large increase in anodic wave IV and a decrease of the anodic wave III. Data related to the current function of waves I–IV (Fig. 1c) for voltammograms where the negative scan was reversed at about −2.8 V are given in Table 2. The peak current for wave II was measured from an extrapolated baseline of the decay of wave I. Generally, an increase in the current function for wave IV and a decrease in the current function for wave III were observed as the scan rate increased. Voltammograms of TCPO solutions where the potential in the negative scan was held for several seconds at values well before the appearance of wave II showed no significant increase in the anodic wave IV.

The electrochemical rate for waves I and III suggest that TCPO is reduced quasi-reversibly to the anion radical:

$$TCPO + e^- \rightleftarrows TCPO^{\cdot -} \qquad (6)$$

TABLE 2

Current functions of waves in TCPO system at differenct scan rates [a]

Scan rate /mV s^{-1}	$i_p^{I} v^{-1/2}/\mu A$ $s^{1/2}$ $mV^{-1/2}$	$i_p^{II} v^{-1/2}/\mu A$ $s^{1/2}$ $mV^{-1/2}$	$i_p^{III} v^{-1/2}/\mu A$ $s^{1/2}$ $mV^{-1/2}$	$i_p^{IV} v^{-1/2}/\mu A$ $s^{1/2}$ $mV^{-1/2}$
10	2.75	2.34	2.5	0.09
20	2.46	2.24	2.21	0.19
50	2.23	1.94	1.45	0.71
100	2.2	1.77	1.05	0.8
200	2.2	1.55	1.02	1.27
500	1.85	-	0.85	1.41

[a] Solution was 5 mM in TCPO, 0.1 M $TBABF_4$ in AN + benzene (2:1 v/v), under vacuum.

The absence of hyperfine splitting in the ESR spectrum suggests that the odd electron density in $TCPO^{\cdot -}$ is probably highest in the carbonyls, i.e., $TCPO^{\cdot -}$ can be considered predominantly in the semidione form [22]. From coulometry, $TCPO^{\cdot -}$ is not very stable at longer times and reacts (probably with impurities) to produce 2,4,6-trichlorophenoxide as one of the decomposition products. The second reduction wave at -2.52 V vs. Ag qre (wave II) is probably related to the reduction of

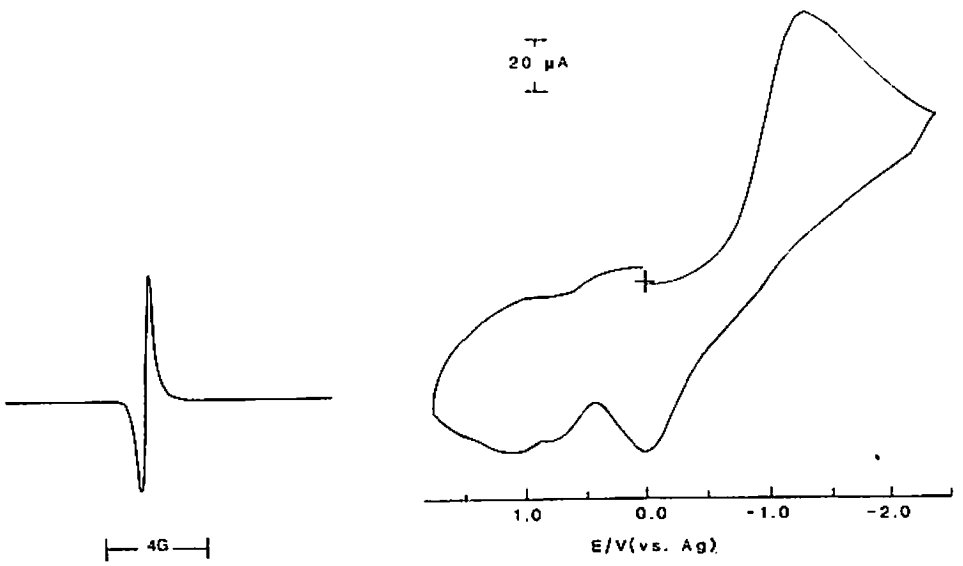

Fig. 6. ESR spectrum of TCPO radical anion produced by electroreduction of 2 mM TCPO solution containing 0.1 M $TBABF_4$ in AN + benzene under vacuum. Spectrometer conditions: modulation amplitude, 0.8 Gs; power, 15 mW; sweep time, 8 min.

Fig. 7. Cyclic voltammogram of a 5 mM TCP solution in AN + benzene (2:1 v/v) + 0.1 M $TBABF_4$, under vacuum; scan rate, 10 V s^{-1}.

TCPO$^{\cdot}$ to TCPO^{2} followed by fast decomposition to 2,4,6-trichlorophenoxide. To understand better the nature of the phenoxide wave, a brief study of the electrochemistry of trichlorophenol (TCP) was undertaken.

Electrochemistry of TCP under vacuum

A typical CV of TCP in AN + benzene (2:1 v/v), containing 0.1 *M* $TBABF_4$ under vacuum is shown in Fig. 1d. Cyclic voltammetric data for waves V and VI at different scan rates are listed in Table 3. During the reduction (V), evolution of a gas (presumably H_2) was observed. Thus, the reduction of the proton on the phenol occurs to produce phenoxide (oxidized in wave VI). The decrease of the current function for wave V as the scan rate increases may be related to the catalytic regeneration of the reactant by reaction with trace water according to the following reaction scheme:

$$ROH + e^- \rightarrow RO^- + \tfrac{1}{2} H_2 \qquad \text{(wave V)} \qquad (7)$$

$$RO^- + HS \rightarrow ROH + S^- \qquad (8)$$

$$RO^{\cdot} - e^- \rightarrow RO^{+} \rightarrow \text{products} \qquad \text{(wave VI)} \qquad (9)$$

R = 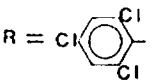 HS = acidic species, e.g., H_2O

The current function for wave VI increases as the scan rate increases over the range of 10 to 500 mV/s, but at $v > 1$ V/s, the current function for wave VI decreases as v increases, and finally the wave disappears (Fig. 7) as new anodic waves appear. This behavior suggests that the electrochemistry of TCP is more complicated than the simple EC′ scheme shown. We must add that, particularly at slow rates, the CV i_p values can be affected by convective effects that are more pronounced (because

TABLE 3

Cyclic voltammetric results for TCP [a]

Scan rate	$i_p^{V} v^{-1/2}/\mu A$ $s^{1/2}\ mV^{-1/2}$	$i_p^{VI} v^{-1/2}/\mu A$ $s^{1/2}\ mV^{-1/2}$
10	1.5	0.13
20	1.41	0.31
50	1.4	0.71
100	1.32	0.82
200	1.26	0.81
500	1.16	1.0
1000	0.95	0.6
2000	0.96	0.3
5000	0.89	0.2

[a] Solution was 5 m*M* in TCP, 0.1 *M* $TBABF_4$ in AN + benzene (2:1 v/v), under vacuum.

of unavoidable vibrations) for cells connected to the vacuum line. However, a more complete investigation of the electrochemical behavior of TCP was beyond the scope of this work, since our interest was focussed primarily on the identification of the species responsible for wave IV in Fig. 1a. The voltammetric results for TCPO (Table 2) and TCP (Table 3) solution under vacuum show that the anodic wave IV in Fig. 1a is associated with the oxidation of the phenoxide produced by slow $TCPO^{\cdot -}$, or rapid $TCPO^{2-}$, decomposition. This oxidation is probably complicated by reaction of phenoxide with proton sources to give TCP, and perhaps by other reactions, e.g., dimerization [27,28]. Further studies are needed for a complete understanding of this mechanism.

Electrochemistry of TCPO in the presence of oxygen

The TCPO system is very sensitive to the addition of small amounts of O_2. Figure 8 shows a cyclic voltammogram of a 6 m*M* TCPO solution in AN + benzene (2 : 1 v/v) + 0.1 *M* $TBABF_4$, containing a very small amount of oxygen, and Fig. 9 shows the effect of increasing amounts of oxygen added to a 2.3 m*M* TCPO solution. With the addition of O_2, the first TCPO reduction wave at −1.1 V vs. Ag becomes irreversible and a new wave (II′) at −1.44 V appears. The anodic wave IV, which is very small in the absence of O_2, increases with increasing amounts of O_2. Data from Fig. 9 are listed in Table 4. As the amount of oxygen in solution increases, waves II′ and IV increase, while wave I remains practically constant and shifts to more positive potentials. A 0.1 *M* $TBABF_4$ solution in AN + benzene saturated with O_2 shows a reduction peak at about −1.4 V vs. Ag qre, corresponding to wave II′ and

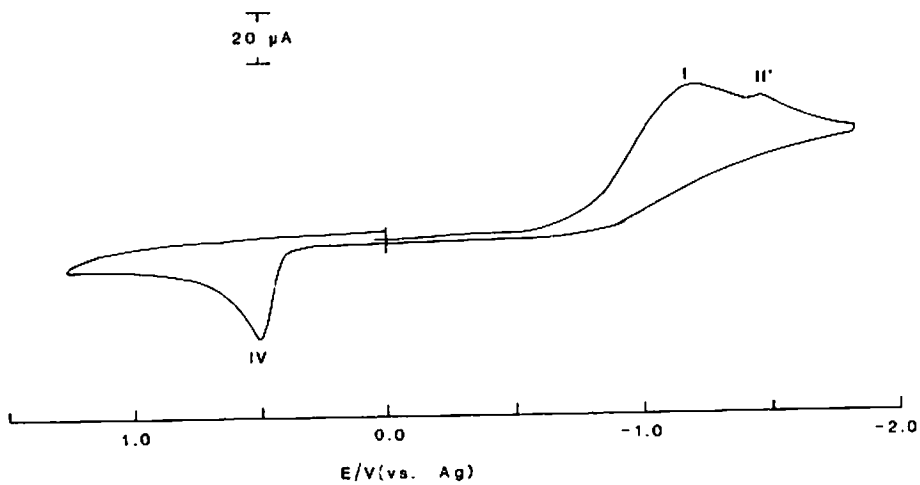

Fig. 8. Cyclic voltammogram of a 6 m*M* TCPO solution in AN + benzene (2 : 1 v/v) + 0.1 *M* $TBABF_4$ containing a small amount of oxygen. Scan rate, 100 mV s^{-1}, Pt disk (0.026 cm^2).

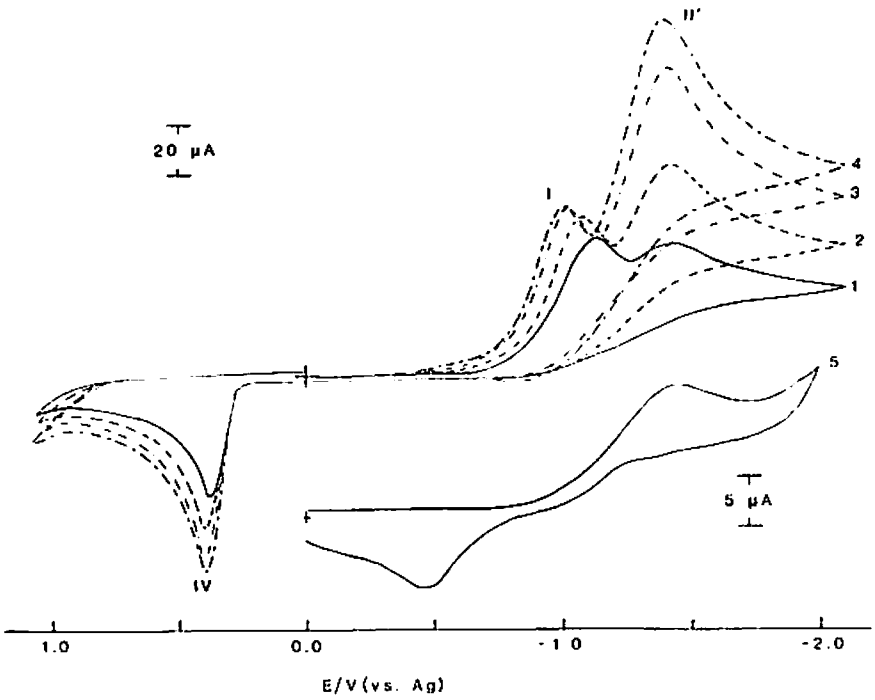

Fig. 9. Cyclic voltammograms with increasing amount of O_2 (1 to 4) added to a 2.3 m*M* TCPO solution containing 0.1 *M* $TBABF_4$ in AN + benzene (2:1 v/v). Scan rate, 100 mV s^{-1}; Pt disk (0.026 cm^2). (5) CV of a 0.1 *M* $TBABF_4$ solution in AN + benzene (2:1 v/v) containing oxygen. Scan rate, 100 mV s^{-1}; Pt disk (0.03 cm^2).

TABLE 4

Cyclic voltammetric results for a TCPO solution containing increasing amounts of O_2 [a,b]

Curve	i_p^I/μA	$i_p^{II'}$ [c]/μA	i_p^{IV}/μA	E_p^I [d]/V	$E_p^{II'}$ [d]/V	Approximate oxygen conc. [e]/ m*M*
1	52	36	43	−1.13	−1.44	2
2	56	61	56	−1.08	−1.43	4
3	58	101	68	−1.02	−1.405	6
4	57	129	72	−1.01	−1.395	8

[a] Solution was 2.3 m*M* in TCPO + 0.1 *M* $TBABF_4$ in AN + benzene (2:1 v/v).

[b] $v = 100$ mV/s.

[c] The current was calculated from the decay of wave I.

[d] Potentials are vs. Ag qre.

[e] O_2 concentration was obtained by calibration with the CV of a 0.1 *M* $TBABF_4$ solution in AN + benzene (2:1 v/v) containing oxygen.

the formation of $O_2^{\cdot-}$ (Fig. 9, curve 5). Table 5 shows the values of the current function for waves I–IV at different scan rates, for the same oxygen concentration in a 7 m*M* TCPO solution. The current function for wave I is essentially constant while the current function of wave IV increases as v increases. The same behavior was previously observed for the anodic wave at +0.52 V vs. Ag qre in TCPO solutions (Table 2, wave IV) and for wave VI in TCP solutions (Table 3) under vacuum. On the basis of these results we propose the following mechanism for the reduction of TCPO in the presence of O_2:

$$TCPO + e^- \rightleftarrows TCPO^{\cdot-} \qquad \text{(wave I)} \tag{10}$$

$$O_2 + e^- \rightleftarrows O_2^{\cdot-} \qquad \text{(wave II')} \tag{11}$$

$$TCPO^{\cdot-} + O_2^{\cdot-} \rightarrow (TCPO\text{–}O_2)^{2-} \xrightarrow{\text{fast}} 2\,RO + 2\,CO_2 \tag{12}$$

as well as the reactions in eqns. (7)–(9). Reaction (12) must be very rapid, since only a small amount of O_2 eliminates the anodic reversal waves for reactions (10) and (11) and increases the current function for wave IV. This reaction could also occur in an ECE sequence, such as

$$O_2 + TCPO^{\cdot-} \rightarrow TCPO + O_2^{\cdot-} \rightarrow TCPO\text{–}O_2^- \tag{13}$$

$$TCPO\text{–}O_2^- + e^- \rightarrow (TCPO\text{–}O_2)^{2-} \tag{14}$$

followed by reaction (12) or with cleavage of the intermediate $TCPO\text{–}O_2^-$

$$TCPO\text{–}O_2^- \rightarrow RO^- + X^{\cdot} \tag{15}$$

$$X^{\cdot} + e^- \rightarrow X^- \rightarrow RO^- + 2\,CO_2 \tag{16}$$

Electrogenerated chemiluminescence

A CV of a 6 m*M* TCPO solution containing 3 m*M* DPA and 0.1 *M* $TBABF_4$ in AN + benzene under vacuum is shown in Fig. 10. DPA radical anion ($DPA^{\cdot-}$) seems to affect the stability of $TCPO^{\cdot-}$, since the current ratio, i_{pa}/i_{pc}, for TCPO reduction is close to 1 and the anodic wave at +0.52 V is very small, if the potential is reversed after TCPO reduction wave (curve a, Fig. 10), while a large decrease in

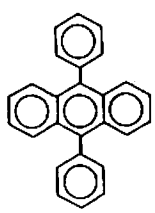

DPA

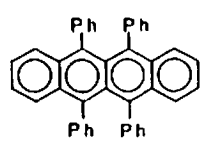

Rubrene

TABLE 5

Current functions for waves I–IV in a TCPO solution containing O_2 [a]

Scan rate, v/mV s^{-1}	$i_p^{I} v^{-1/2}$/μA s$^{1/2}$ mV$^{-1/2}$	$i_p^{II} v^{-1/2}$ [b]/μA s$^{1/2}$ mV$^{-1/2}$	$i_p^{IV} v^{-1/2}$/μA s$^{1/2}$ mV$^{-1/2}$
50	1.8	3.99	2.5
100	1.95	3.25	2.85
200	1.5	3.15	3.18
500	1.8	3.18	3.44
1000	–	3.1	–

[a] Solution was 7 mM TCPO + 0.1 M $TBABF_4$ in AN + benzene 2:1 (v/v).
[b] The current intensities were calculated from the decay of wave I

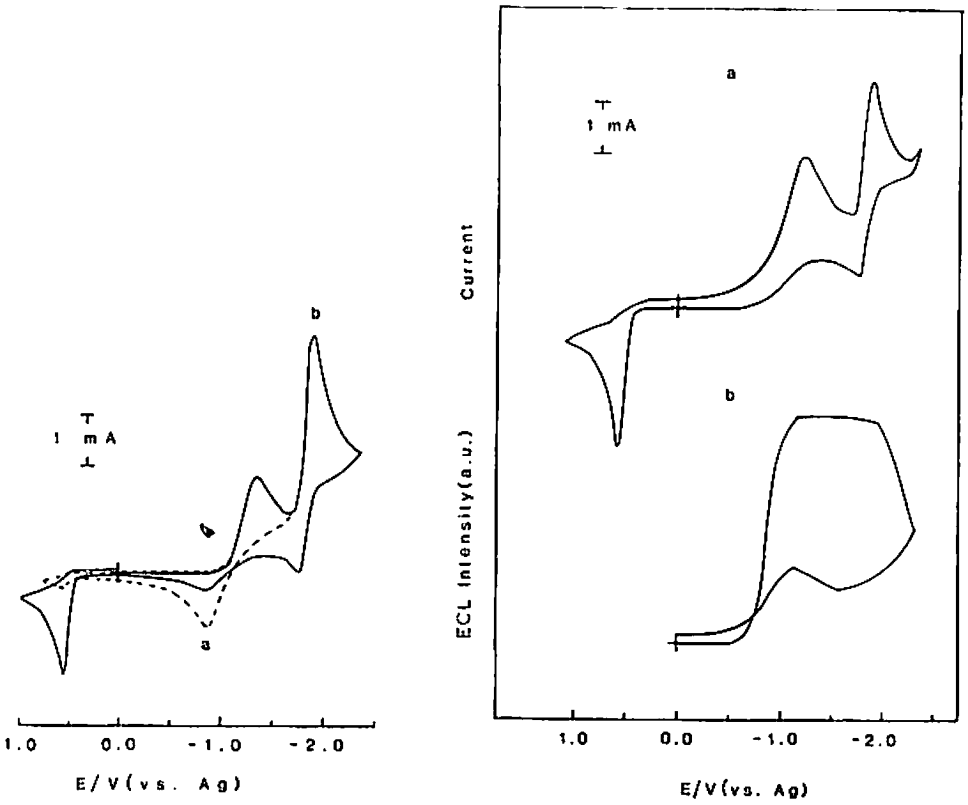

Fig. 10. Cyclic voltammogram of a 6 mM TCPO solution in AN + bezene (2:1 v/v) + 0.1 M $TBABF_4$ containing 3 mM DPA under vacuum. (a) Scan reversed after TCPO reduction peak; (b) Scan reversed after DPA reduction peak. Scan rate, 100 mV s^{-1}; Pt flag (0.8 cm^2).

Fig. 11. (a) Cyclic voltammogram of a 5 mM TCPO + 3 mM DPA solution in AN + benzene + 0.1 M $TBABF_4$, containing O_2. Scan rate, 100 mV s^{-1}; Pt flag (0.8 cm^2). (b) ECL intensity as a function of applied potential for solution in (a). Scan rate, 100 mV s^{-1}.

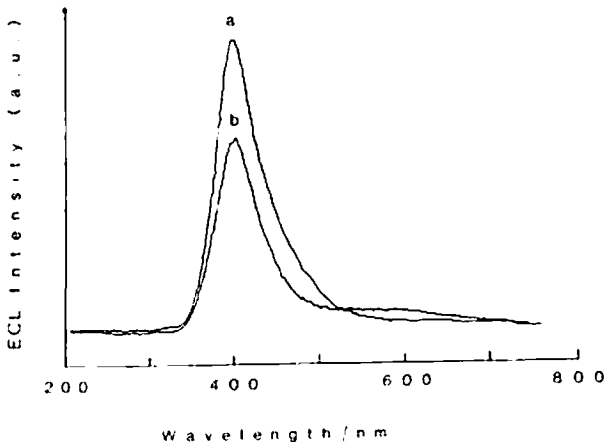

Fig. 12. (a) ECL spectrum for a 3 m*M* DPA solution in AN + benzene (2 : 1 v/v) + 0.1 *M* $TBABF_4$, obtained by pulsing the potential between −2.3 V and +1.6 V vs. Ag qre. (b) ECL spectrum of 5 m*M* TCPO + 3 mM DPA solution in AN + benzene (2 : 1 v/v) + 0.1 *M* $TBABF_4$, containing O_2. The spectrum was obtained by stepping the potential to −1.3 V vs. Ag qre.

i_{pa}/i_{pc} and an increase of the anodic wave IV is observed in Fig. 10 (curve b). This is probably caused by the reaction of $DPA^{\cdot}$ with $TCPO^{\cdot-}$ to form the TCPO dianion (redox catalysis [29]), which then decomposes rapidly to $TCP^{\cdot-}$. When the solution used in Fig. 10 was opened to the air and O_2 was bubbled into the cell, a broad wave appeared, centered at about −1.2 V vs. Ag qre, in the region where the TCPO reduction wave is located (Fig. 11a). This broad wave is due to the superimposition of 2 waves, the TCPO and O_2 reduction waves, as discussed in the previous section. Figure 11b shows the ECL light intensity for the solution in Fig. 11a, when the potential was scanned from 0.0 V to −2.3 V vs. Ag qre at 100 mV/s. Intense light emission was observed at potentials corresponding to the broad wave at −1.2 V in Fig. 11a. The light is easily visible to the dark-adapted eye. No light was detected under these conditions (negative scan) when only DPA or TCPO was in solution. The spectrum of the emitted light is shown in Fig. 12, together with the ECL spectrum of a 3 m*M* DPA solution, obtained by pulsing the potential between −2.3 V and +1.6 V vs. Ag qre. The ECL intensity is very sensitive to the amount of oxygen present in solution. One or two freeze–pump–thaw cycles were not sufficient for a complete elimination of oxygen from solution. The O_2 still present was responsible for a clearly detectable light signal similar to the one shown in Fig. 11b, even though O_2 could not be identified on the CV. No light was detected when the system was carefully deoxygenated with several freeze–pump–thaw cycles. When the same experiment was performed in a TCPO solution containing rubrene or $Ru(bpy)_3^{2+}$ as luminescer instead of DPA, similar results were obtained. The light emitted was characteristic of the particular luminescer present in solution. Note that for both DPA and rubrene (F) emission occurs before reduction of F to the radical

anion takes place. Among the three luminescers tested, $Ru(bpy)_3^{2+}$ showed the lowest ECL intensities, being ca. two orders of magnitude less intense than DPA emission. As in previous studies of oxalate ester chemiluminescence [2–6], an intermediate formed in the decomposition of the adduct $(TCPO{-}O_2)^{2-}$ in reaction (12) can produce an excited state of the emitter, i.e.,

$$(TCPO{-}O_2)^{2-} + F \rightarrow 2\ RO^- + 2\ CO_2 + F^* \quad (17)$$

$$F^* \rightarrow F + h\nu \quad (18)$$

Note that it is species F and not its radical anion that is involved in the ECL reaction. In fact at potentials where the radical anion (e.g., $DPA^{\cdot-}$) is produced, the ECL intensity decreases (Fig. 11b), probably because the radical anion promotes further reduction of $TCPO^{\cdot-}$ with subsequent rapid decomposition. While we have no details about the structure of $(TCPO{-}O_2)^{2-}$ or the nature of the reaction producing DPA* (eqn. 14), by analogy to previous chemiluminescence studies, we propose the following:

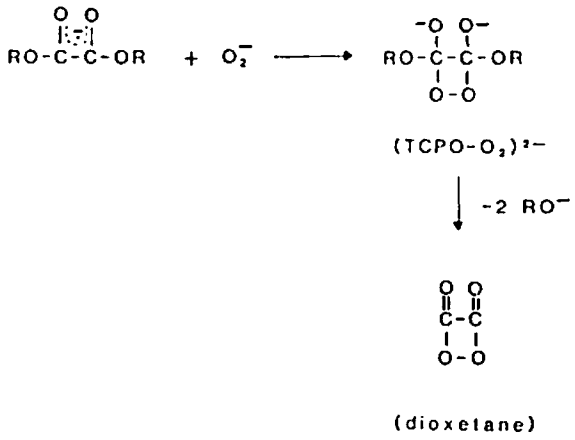

or alternatively, the intermediate, $X^{\cdot-}$, in eqn. (16) would produce dioxetane. The dioxetane reacts with DPA to yield DPA* and 2 CO_2 molecules.

CONCLUSIONS

TCPO is reduced quasi-reversibly at a platinum electrode, under vacuum. The product of the reduction, $TCPO^{\cdot-}$, is stable on the cyclic voltammetric time scale, but it probably reacts with trace impurities in the system or with oxygen radical anion on the coulometric time scale to produce trichlorophenoxide ion. The reaction of $O_2^{\cdot-}$ with $TCPO^{\cdot-}$ is very rapid and leads to the same decomposition products as those previously observed in the chemiluminescent reaction between TCPO and H_2O_2. ECL is observed in TCPO solutions containing oxygen and a luminescer

(DPA, rubrene, $Ru(bpy)_3^{2+}$) at potentials corresponding to TCPO and O_2 reduction. The ECL spectrum is characteristic of the luminescer. TCPO solutions show interesting possibilities for the electrochemical determination of trace amounts of O_2 by detection of the electrogenerated chemiluminescence. Further studies are needed for a more quantitative appraisal of the TCPO system as a detector for O_2.

ACKNOWLEDGEMENT

The support of this research by the Army Research Office is gratefully acknowledged. We are grateful to a reviewer for suggesting the possibility of a ECE mechanism in dioxetane formation.

REFERENCES

1 E.A. Chandross, Tetrahedron Lett., (1963) 761.
2 A.G. Mohan in J.G. Burr (Ed.), Chemi- and Bioluminescence, Marcel Dekker, New York, 1985, p. 245.
3 M.M. Rauhut, L.J. Bollyky, B.G. Roberts, M. Loy, R.H. Whitman, A.V. Iannotta, A.M. Semsel and R.A. Clarke, J. Am. Chem. Soc., 89 (1967) 6515.
4 S.S. Tseugo, A.G. Mohan, L.G. Haines, L.S. Vizcarra and M.M. Rauhut, J. Org. Chem., 44 (1979) 4113.
5 (a) M.M. Rauhut, Acc. Chem. Res., 2 (1969) 80; (b) M.M. Rauhut, B.G. Roberts, D.R. Maulding, W. Bergmark and R. Coleman, J. Org. Chem., 40 (1975) 330.
6 L.J. Bollyky, R.H. Whitman, B.G. Roberts and M.M. Rauhut, J. Am. Chem. Soc., 89 (1967) 6523.
7 P. Lechtken and N.J. Turro, Mol. Photochem., 6 (1974) 95.
8 F. McCapra, Prog. Org. Chem., 8 (1973) 231.
9 G.B. Schuster, Acc. Chem. Res., 12 (1979) 366.
10 (a) M.M. Chang, T. Saji and A.J. Bard, J. Am. Chem. Soc., 99 (1977) 5399; (b) I. Rubinstein and A.J. Bard, J. Am. Chem. Soc., 103 (1981) 512; (c) I. Rubinstein, C.R. Martin and A.J. Bard, Anal. Chem., 55 (1983) 1580; (d) D. Ege, W.G. Becker and A.J. Bard, Anal. Chem., 56 (1984) 2413.
11 M.M. Rauhut in M. Grayson (Ed.), Chemiluminescence, Encyclopedia of Chemical Technology, 3rd ed., Vol. 5, Wiley, New York, 1979, pp. 416–450.
12 K. Honda, K. Miyeguchi and K. Imei, Anal. Chim. Acta, 177 (1985) 103.
13 R.W. Sigvardson and J.W. Birks, Anal. Chem., 55 (1983) 432.
14 M.L. Grayeski and W.R. Seitz, Anal. Biochem., 136 (1984) 277.
15 P.A. Sherman, J. Holzbecker and D.E. Ryan, Anal. Chim. Acta, 97 (1978) 21.
16 R. Honda, R. Miyaguchi and K. Imai, Anal. Chim. Acta, 177 (1985) 111.
17 A.G. Mohan and N.J. Turro, J. Chem. Educ., 51 (1974) 528.
18 F.J. Alvarez, N.J. Parekh, B. Matuszewski, R.S. Givens, T. Higuchi and R.L. Schowen, J. Am. Chem. Soc., 108 (1986) 6435 and references therein.
19 (a) G.J. De Jong, N. Lammers, F.J. Spruit, R.W. Frei and U.A.H. Brinkman, J. Chromatogr., 353 (1986) 249; (b) K.W. Sigvardson, J.M. Kennish and J.W. Birks, Anal. Chem., 56 (1986) 1096.
20 P. Van Zoonen, D.A. Kamminga, C. Gooijer, N.H. Vethorst and R.W. Frei, Anal. Chim. Acta, 174 (1985) 151.
21 L. Eberson and K. Nyberg in A.J. Bard and H. Lund (Eds.), Encyclopedia of Electrochemistry of the Elements, Vol. 12, Marcel Dekker, New York, 1978, Ch. 2.
22 A.V. Ilyasov, Yu.-M. Kargin, Ya. A. Levin, I.D. Morozova, N.N. Sotnikova, V. Kh. Ivanova and R.T. Sofin, Izv. Akad. Nauk SSSR, Ser. Khim., 4 (1968) 736.
23 J. Voss, Tetrahedron, 27 (1971) 3753.
24 I.B. Goldberg and A.J. Bard, J. Phys. Chem., 75 (1971) 3781.
25 A.J. Bard and L.R. Faulkner, Electrochemical Methods, Wiley, New York, 1980, (a) p. 143 (b) p. 222.

26 (a) J.O. Howell and R.M. Wightman, Anal. Chem., 56 (1984) 524; (b) M. Fleischmann, F. Lasserre, J. Robinson and D. Swan, J. Electroanal. Chem., 177 (1984) 115; (c) A. Fitch and D.H. Evans, J. Electroanal. Chem., 202 (1986) 83.
27 F.W. Steuber and K. Dimroth, Chem. Ber., 99 (1966) 258.
28 I. Papouchado, R.W. Sandford, G. Petrie and R.N. Adams, J. Electroanal. Chem., 65 (1975) 275.
29 See, e.g. (a) C.P. Andrieux, C. Blocman, J.M. Dumas-Bouchiat and J.M. Savéant, J. Am. Chem. Soc., 101 (1979) 3431; (b) C.P. Andrieux, I. Gallardo, J.M. Savéant and K.B. Su, J. Am. Chem. Soc., 108 (1986) 638 and references therein.